

## SUPPLEMENTAL INFORMATION

### Detailed methods

#### *Mouse strains.*

Mice were housed in a 12:12 light-dark cycle and chow and water were provided *ad libitum*, when not otherwise specified. Strains purchased include: C57BL/6 (JAX:000664), *Adipoq-Cre* (JAX:028020), *Isg15<sup>-/-</sup>* (JAX: 010486) and Cas9 knock-in mice (JAX: 024857).

IRF3-2D mice were generated by introducing the 3XFlag-IRF3-2D transgene into the ROSA26 locus downstream of a “STOP” cassette consisting of multiple polyadenylation signals flanked by loxP sites. The IRF3-2D coding sequence was amplified using murine 3Xflag-IRF3-2D-pCDH-CMVMCS-EF1-puro construct (1) with the addition of MluI and NsiI restriction sites and ligated into the BirA-RanGap-TRAP vector (2). Primers used for cloning are: forward 5'-GACACGCGTACCATGGATTACAAGGATGACGACGATAAGATGGAAACCCCGAAACCG-3' and reverse 5'-GACATGCATTTCAGATATTTCCAGTGGCCTG-3'. The vector was linearized by KpnI digestion and the purified product was introduced into C57BL/6N ES cells. Correctly targeted ES cell clones were identified by long-range PCR screen (3). The following primers were used to screen the 5' insertion site: 5'-GCCAAGTGGGCAGTTTACCG-3' (outside of the 5'-arm) and 5'-TAGGTAGGGGATCGGGACTCT-3' (in the CAG). For the 3' insertion site, the primers used were: 5'-GCCAGCTCATTCTCCCACTC-3' and 5'-GGCATGGCAATGTTCAAGCAG-3' (outside of 3'-arm). Chimeric mice were generated by microinjection of ES cells into blastocysts, and germ-line transmission was confirmed by testing the presence of ROSA26 transgene DNA into genomic DNA by PCR using two pairs of the following primers: forward 5'-GCAGCCCAAGCTAGATCGAAT-3', reverse 5'-TTGACACGTCCGGCTTATCC-3' for the transgene and forward 5'-CCTAGCTGTCACCAACCCTTT-3', reverse 5'-GACGAAGAGCATCACAAAGGAG-3' for the wild-type.

The IRF3 floxed mice were generated by using a gene targeting vector designed to place LoxP sites flanking exons 4-6. Murine C57BL/6 embryonic stem cells were transfected, and integration of the genomic construct at the predicted site within the *Irf3* locus was confirmed by long distance PCR using primers external to the targeted region (3' homologous arm and 5' homologous arm). Following ES cell expansion and karyotyping, selected clones were microinjected into C57BL/6 blastocysts and implanted into pseudo-pregnant female mice. Male germ line chimeras carrying an *Irf3* floxed allele were backcrossed with wild-type C57BL/6N females. Heterozygous F1 progeny were crossed to Flpe line (B6.Cg-Tg(ACTFLPe)9205Dym/J) to remove the selection

cassette and obtain the floxed allele only. Use of mice was in accordance with protocols approved by the TAMU Institutional Animal Care and Use Committee and following the National Institutes of Health guidelines for laboratory animal use. These new mouse lines will be available from the Jackson Laboratory: *Irf<sup>flox</sup>* [JAX#036260] and IRF3-2D [JAX#036261].

#### *Metabolic studies.*

Eight-week-old male mice were fed a high-fat diet (Research Diets, D12492) or standard diet (chow) at an ambient temperature of 22 °C or thermoneutrality (30 °C) for 16 weeks. Body weight and food intake were measured weekly. Fat and lean mass was determined by EchoMRI-100. Oxygen consumption and energy expenditure was measured using the Comprehensive Laboratory Animal Monitoring System (CLAMS). Data were normalized to lean body mass determined by EchoMRI. CL 316,243 (Sigma) was intraperitoneally injected daily into mice at 1mg/kg for 5 days, with tissues collected four hours after last injection.

#### *Glucose and Insulin Tolerance Tests.*

For glucose tolerance tests (GTT), mice were fasted overnight and then injected intraperitoneally with glucose (1.5 g per kg body weight). For insulin tolerance tests (ITT), mice were fasted for 6 hrs and then injected intraperitoneally with insulin (Humulin, Eli Lilly; 0.75 U per kg body weight for mice on chow and 1.5 U per kg body weight for mice on HFD). Blood samples were collected from a tail nick at the indicated time points, and glucose levels were measured using test strips (OneTouch).

#### *Human studies.*

A total of 48 nondiabetic and 45 Type 2 diabetic individuals were recruited in the study. Anthropometric and clinical measurements were taken by measuring of height and weight using calibrated portable electronic weighing scales and portable inflexible height measuring bars. BMI was calculated using the standard BMI formula, body weight (kg)/height<sup>2</sup> (m<sup>2</sup>). Peripheral blood was collected from overnight-fasted individuals and analyzed for fasting glucose, glycated hemoglobin (HbA1c), fasting insulin, and lipid profile using standard clinical laboratory procedures. Clinical parameters are presented in **Table S3**.

#### *RNA isolation and qRT-PCR.*

Total RNA was extracted from cells or tissues using Direct-zol RNA MiniPrep kit (ZYMO Research) or Trizol reagent (Invitrogen). Reverse transcription was performed with 1µg of total RNA using High-Capacity cDNA Reverse Transcription Kit (Thermo Fisher). qRT-PCR was performed on an ABI PRISM 7500 (Applied Biosystems). Melting curve analysis was carried out to confirm the RT-

PCR products. Statistical analysis was performed using ddct method with TBP primers as control (see primer sequences in **Table S4**).

#### *RNA-seq.*

For RNA-seq library construction, primary adipocyte RNA (100ng) was treated with the Ribo-Zero rRNA removal kit (Epicentre) to deplete ribosomal RNA and converted into double stranded cDNA using NEBNext mRNA Second Strand Synthesis Module (E6111L). cDNA was subsequently tagged and amplified for 12 cycles by using Nextera XT DNA Library Preparation Kit (Illumina FC-131). Sequencing libraries were analyzed Qubit and Agilent Bioanalyzer, pooled at a final concentration of 12pM, and sequenced on a HiSeq2500.

For RNA-seq analysis, sequencing reads were demultiplexed using bcl2fastq and aligned to the mm10 mouse genome using HISAT2 (4). PCR duplicates and low-quality reads were removed by Picard (<https://broadinstitute.github.io/picard>). Filtered reads were assigned to the annotated transcriptome and quantified using feature Counts (5). Normalization and differential expression analysis were performed using EdgeR (6). For differential gene expression analysis, we only tested genes that were detected in at least two samples with  $\log_2\text{CPM} \geq 2$ . Genes were considered significant if they passed a fold change (FC) cutoff of  $\log_2\text{FC} \geq 1$  and a false discovery rate (FDR) cutoff of  $\text{FDR} \leq 0.05$ . Morpheus (<https://software.broadinstitute.org/morpheus/>) was used for heatmap visualization. Volcano plots was generated in R. The volcano plots were generated with an easy-to-use, interactive R Shiny app that we developed for public use ([https://bdawes.shinyapps.io/volcano\\_plotter/](https://bdawes.shinyapps.io/volcano_plotter/)), which also includes functionality for depicting MA and abundance plots. Gene set enrichment analysis was performed using DAVID Bioinformatics Resources 6.8 (7). Data are presented in **Table S1**. The accession number for the RNA-seq dataset reported in this paper is GEO: GSE155019.

#### *Cold tolerance test.*

Mice were pre-acclimatized at thermoneutrality (30°C) for two weeks and then shifted to 4°C. Body temperature was measured with a rectal probe (Physitemp, RET3) and a reader (Physitemp, BAT-12).

#### *Immunoblotting.*

For immunoblotting analyses, tissues and cells were lysed in RIPA buffer containing protease and phosphatase inhibitors (Thermo Fisher). Protein levels were quantified using BCA protein assay kit (Thermo Fisher) and lysates containing equal amount of protein were subjected to SDS-PAGE,

transferred to polyvinylidene fluoride (PVDF) membranes, followed by incubations with primary and secondary antibodies. Key antibodies: rabbit monoclonal anti-IRF3 (#4302), rabbit polyclonal anti-HSP90 (#4874), rabbit monoclonal anti-PKM2 (#4053), rabbit monoclonal anti-PFKP (#8164), rabbit monoclonal anti-HK1 (#2024), rabbit monoclonal anti-HK2 (#2867), rabbit monoclonal anti-GAPDH (#5174), mouse IgG (#5873) all from Cell Signaling Technology; rabbit polyclonal anti-LDHA (#19987-1-AP) from Proteintech; and rabbit polyclonal anti-HA (#H6908) and mouse monoclonal anti-FLAG (#M8823) from Sigma-Aldrich. Uncut immunoblots are shown in the Supplemental Data.

#### *Immunostaining.*

For immunostaining, adipose tissues collected from mice were immediately fixed in 10% formalin, incubated overnight at 4°C, and washed with 70% ethanol. Formalin-fixed, paraffin-embedded tissues were stained with H&E or processed for IHC. For IHC, sections of formalin-fixed, paraffin-embedded adipose tissues were incubated with anti-UCP1 antibody (Abcam ab10983, 1:200) overnight at 4°C. After washing, bound antibody was detected with a labeled polymer-HRP (Envision Plus kit: Agilent) using DAB chromogen.

#### *Hepatic TG content assay.*

Hepatic TG content was assessed following lipid extraction as previously described (8). Briefly, snap-frozen liver samples were weighed and homogenized in ten volumes of ice-cold PBS. Two-hundred microliters of the homogenate was transferred into 1,200  $\mu$ l of chloroform: methanol (2:1; v/v) mixture followed by vigorous vortex for 30 s. One-hundred microliters of ice-cold PBS was then added into the mixture and mixed vigorously for 15 s. The mixture was then centrifuged at 4,200 rpm for 10 min at 4°C. Two-hundred microliters of the organic phase (bottom layer) was transferred into a new tube and evaporated for dryness. Two-hundred microliters of 1% Triton X-100 in ethanol was used to dissolve the dried lipid with constant rotation for 2 h. Triglyceride content was determined using the Infinity Triglycerides reagent (Thermo Scientific), based on manufacturer's instructions.

#### *Separation of SVF and adipocyte fraction.*

Adipose tissue fractionation was carried out as previously described (1). Briefly, mouse iWAT was minced and digested in buffer (collagenase D [Sigma, 2.5 U/ml], Dispase II [Sigma, 2.4 U/ml], CaCl<sub>2</sub> [10 mM] in PBS) for 45 min at 37°C in a shaking water bath. The cell suspension was then passed through a 100  $\mu$ m mesh and spun at 600g for 5min. Floating adipocytes were collected for RNA or protein extraction, while the cell pellet was resuspended in PBS, passed

through a 40 µm mesh and plated prior to in vitro differentiation, or lysed with RIPA buffer for immunoblotting or with Trizol for RNA isolation.

*Primary beige adipocyte culture.*

Beige adipocyte differentiation was induced by treating confluent SVF cells with DMEM/F-12 containing 10% FBS, 0.5 mM isobutylmethylxanthine, 125 nM indomethacin, 2 µg/ml dexamethasone, 850 nM insulin, 1 nM T3 and 0.5 µM rosiglitazone (all from Sigma). Two days after induction, cells were switched to maintenance medium containing 10% FBS, 850 nM insulin and 1 nM T3. For some experiments, cells were transduced with adenoviral constructs (Cre-GFP Adenovirus, #000023A; GFP Adenovirus, #000541A; mouse USP18-HA Adenovirus, #220205A, all from Applied Biological Materials).

*Seahorse assay.*

For cultured cells, OCR and ECAR were measured using the Seahorse XFe Extracellular Flux Analyzer (Agilent) in a 96-well plate. Primary beige adipocytes were differentiated in 12-well plates, trypsinized, and reseeded in XF96 plates at 2K cells per well at day 6 of differentiation and assayed on day 7 of differentiation. On the day of experiments, cells were maintained in XF assay medium supplemented with 1 mM sodium pyruvate, 2 mM GlutaMAX, and 25-mM glucose. Cells were subjected to mitochondrial stress by adding 2-DG (Sigma; 50 mM) or oligomycin (Millipore; 5 µM) followed by carbonyl cyanide 4-(trifluoromethoxy) phenylhydrazone (FCCP) (Sigma; 5 µM) and antimycin (Sigma; 5 µM).

*Cellular lactate and NAD/NADH assays.*

Cellular lactate and NAD/NADH levels in primary beige adipocyte cell lysates ( $1 \times 10^6$  cell) were measured with a colorimetric lactate assay kit (Abcam #ab65331) and colorimetric NAD/NADH kit (BioVision), respectively. LDH activity was measured using a kit from Abcam (#ab102526).

*AAV injection.*

gRNA (CCGGAAGCCTCGGCGCCTGA) targeting exon1 of the mouse *Herc6* gene was cloned into 1179\_pAAV-U6-BbsI-gRNA-CB-EmGFP plasmid (Addgene plasmid #89060). *Herc6* gRNA-containing plasmid or empty vector were packaged in pAAV2/8 particles and verified by Sanger sequencing, then sent to the Boston Children's Hospital Viral Core for AAV production and purification.

For delivery into iWAT, eight-week-old male mice were anesthetized with isoflurane and a longitudinal incision was made in the inguinal skin. To distribute virus to as much of the depot as possible, each iWAT depot received four injections of 20  $\mu$ l AAV-GFP or AAV-Herc6 gRNA at different sites using a Hamilton syringe.

#### *Oil red O staining.*

Cells were washed twice with PBS and fixed with 10% buffered formalin for 30 minutes at room temperature. Cells were then stained with a filtered Oil Red O solution (Sigma; 0.5% Oil Red O in isopropyl alcohol) for 2 hours at room temperature, washed several times with distilled water, and then photographed. For quantitative measurement, the dye is eluted from the cells using 200  $\mu$ l 2-propanol, and absorbance was photometrically determined at 510 nm.

#### *Protein digestion and isobaric labelling.*

Flag elutions (3X-Flag, Sigma) were reduced with TCEP (5mM) and alkylated with iodoacetamide (50 mM) prior to SDS-PAGE separation. Gel bands were cut into 6 gel bands per lane and further diced into 1mm cubes dehydrated with 100% acetonitrile, and each sample was digested with trypsin 0.5 ng in 50 mM ammonium bicarbonate. Digests were extracted and acidified with 50  $\mu$ l of 10% formic acid and subsequently desalted by C18 Stage Tips (3M Empore). Digested peptides were resuspended in 25  $\mu$ l of 200 mM HEPES, pH 8.0. 3 microliters of TMT6 reagents (Thermo Fisher) was added to each solution for 1 hr at room temperature (25 °C). After incubating, the reaction was quenched by adding 1  $\mu$ l of 5% (w/v) hydroxylamine. Labelled peptides were combined and subsequently desalted by C18 Stage Tips.

#### *LC-MS/MS analysis.*

Data were collected using an Orbitrap Fusion Lumos mass spectrometer (Thermo Fisher Scientific, San Jose, CA) coupled with a Proxeon EASY-nLC 1200 LC pump (Thermo Fisher Scientific). TMT labelled peptides were separated onto a 100  $\mu$ m inner diameter microcapillary column packed with 45 cm of Accucore C18 resin (2.6  $\mu$ m, 100 Å, Thermo Fisher Scientific). Peptides were separated using a 3 hr gradient of 6–25% acetonitrile in 0.125% formic acid with a flow rate of ~400 nL/min. Each analysis used an MS<sup>3</sup>-based TMT method as described previously described (9). MS1 data was acquired using a mass range of m/z 400–1400, resolution at 120,000, AGC target of 1 x 10<sup>6</sup>, a maximum injection time 150 ms, dynamic exclusion of 180 seconds for all the peptide measurements in the Orbitrap.

Data dependent MS<sup>2</sup> spectra were acquired in the ion trap with a normalized collision energy (NCE) set at 35%, AGC target set to  $2.0 \times 10^5$  and a maximum injection time of 120 ms. MS3 scans were acquired in the Orbitrap with a HCD collision energy set to 55%, AGC target set to  $1.5 \times 10^5$ , maximum injection time of 200 ms, resolution at 50,000 and with a maximum synchronous precursor selection (SPS) precursors set to 10.

*Mass spectrometry data processing and spectra assignment.*

A compendium of in-house developed software was used to convert acquired mass spectrometric data from the .RAW file to the mzXML format. Erroneous assignments of peptide ion charge state and monoisotopic  $m/z$  were also corrected. SEQUEST algorithm was used to assign MS2 spectra by searching the data against a protein sequence database including Mouse Uniprot Database (downloaded June 2019) and known contaminants such as mouse albumin and human keratins. A forward (target) database component was followed by a decoy component including all listed protein sequences. Searches were performed using a 20 ppm precursor ion tolerance and requiring both peptide termini to be consistent with trypsin specificity. 6-plex TMT labels on lysine residues and peptide N termini (+229.162932Da) were set as static modifications and oxidation of methionine residues (+15.99492 Da) and ISGylation (+721.2569 K) as a variable modification. An MS2 spectra assignment false discovery rate (FDR) of less than 1% was implemented by applying the target-decoy database search strategy. Filtering was performed using a linear discrimination analysis method to create one combined filter parameter from the following peptide ion and MS2 spectra properties: XCorr and  $\Delta C_n$ , peptide ion mass accuracy, and peptide length. Linear discrimination scores were used to assign probabilities to each MS2 spectrum for being assigned correctly and these probabilities were further used to filter the data set with an MS2 spectra assignment FDR to obtain a protein identification FDR of less than 1%. Data are presented in **Table S2**.

*Determination of TMT reporter ion intensities.*

For reporter ion quantification, a 0.003  $m/z$  window centered on the theoretical  $m/z$  value of each reporter ion was monitored for ions, and the maximum intensity of the signal to the theoretical  $m/z$  value was recorded. Reporter ion intensities were normalized by multiplication with the ion accumulation time for both MS2 or MS3 spectrum and adjusted based on the overlap of isotopic envelopes of all reporter ions. Following extraction of the reporter ion signal, the isotopic impurities of the TMT reagent were corrected using the values specified by the manufacturer's specification. Total signal-to-noise values for all peptides were summed for each TMT channel and all values

were adjusted to account for variance and a total minimum signal-to-noise value of 150 was implemented.

#### *Cellular Tracing Experiments.*

Tracing media was prepared from phenol red-, glucose-, glutamine-, sodium pyruvate-, sodium bicarbonate-free DMEM powder (Sigma) supplemented with 10 mM HEPES, pH 7.4, 5 mM D-glucose-<sup>13</sup>C6, 4 mM L-glutamine. 1X10<sup>6</sup> cells were plated 6-well plates and cultured with 2ml culture media. Media was changed to tracing media in WT and *Isg15*<sup>-/-</sup> beige adipocytes. Metabolites were extracted from each well by scraping cells on ice with 125  $\mu$ L cold 80% methanol containing three internal standards: 0.05 ng/ mL thymine-d4, 0.05 ng/ mL inosine-<sup>15</sup>N4, and 0.1 ng/ mL glycocholate-d4. Samples were centrifuged and supernatant was collected.

#### *LC-MS for Metabolomics.*

A total of 10  $\mu$ L metabolite extracts were loaded onto a Luna-HILIC column (Phenomenex) using an UltiMate-3000 TPLRS LC with 10% mobile phase A (20 mM ammonium acetate and 20 mM ammonium hydroxide in water) and 90% mobile phase B (10 mM ammonium hydroxide in 75:25 v/v acetonitrile/methanol). A 10-min linear gradient to 99% mobile phase A were used to separate metabolites, followed by MS analysis with a Q-Exactive<sup>TM</sup> HF-X mass spectrometer (Thermo). Negative ion mode was used with full scan analysis over m/z 70-750 m/z at 60,000 resolution, 1e<sup>6</sup> AGC, and 100 ms maximum ion accumulation time. Additional MS settings were: ion spray voltage, 3.8 kV; capillary temperature, 350°C; probe heater temperature, 320 °C; sheath gas, 50; auxiliary gas, 15; and S-lens RF level 40. Raw data were processed using TraceFinder software (Thermo), and internal standard-calibrated area under curves (AUC) were used to present metabolite abundance.

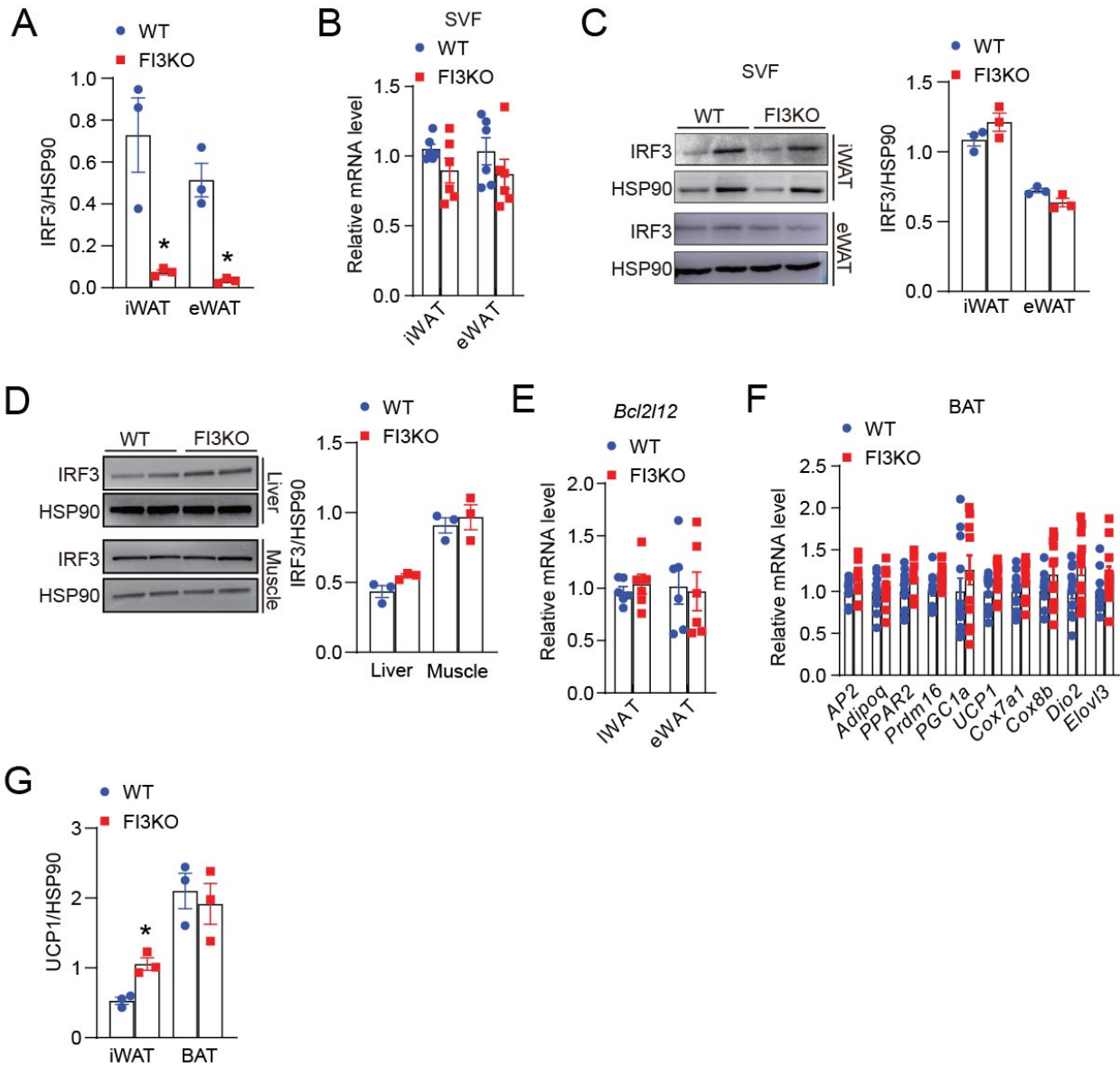
#### *Statistical analysis.*

No statistical methods were used to predetermine sample size. Experiments were not blinded, except cold tolerance tests. Values are presented with mean  $\pm$  SD or mean  $\pm$  SEM, as indicated in figure legends. Statistical analyses were performed using Prism (GraphPad). Statistical significance of differences was determined by unpaired, two-tailed Student's t test (two groups), or two-way ANOVA with Tukey post hoc analysis (more than two groups), with corrected p values < 0.05 considered statistically significant. Asterisks denote corresponding statistical significance \*p < 0.05. The definition of "n" is indicated in the figure legends. For lactate levels, NAD/NADH ratio, qPCR and Western blotting, each sample within each biological replicate corresponds to

one well from a tissue culture plate. For mouse adipose tissue western blotting, each sample corresponds to protein extract from one mouse.

### **Supplemental Figures with figure legends**

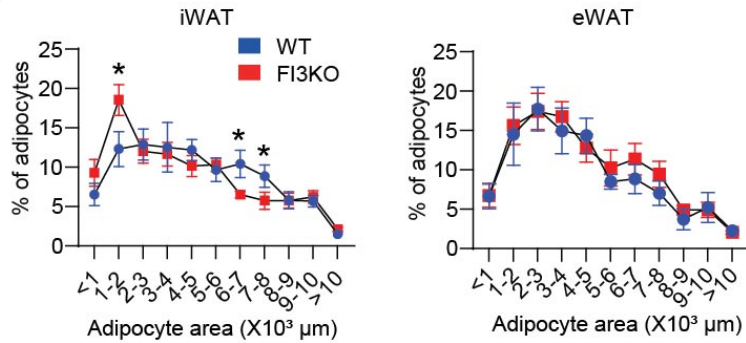
## Supplemental Figure 1



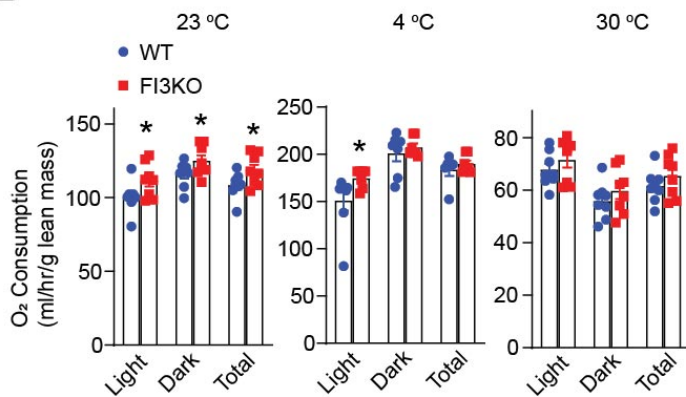
**Supplemental Figure 1. Generation of adipocyte-specific *Irf3* knockout mice.** (A) Quantification of western blot band intensity as described in Figure 1C (n=3). (B) Western blot of IRF3 protein in primary adipocytes and SVFs from iWAT of 8-week old WT mice under room temperature or cold challenge (n=3). (C) *Irf3* expression in SVF from iWAT and eWAT of 8-week old WT and FI3KO male mice (n=6). (D) Western blot of IRF3 protein in liver and muscle from iWAT and eWAT of 8-week old WT and FI3KO male mice (n=3). (E) *Bcl2l12* expression in isolated adipocytes from iWAT and eWAT of 8-week old WT and FI3KO male mice (n=6). (F) Thermogenic gene expression in BAT of chow-fed WT and FI3KO mice after 7 days cold challenge (n=8-10). (G) Quantification of western blot band intensity as described in Figure 1E (n=3). Statistical comparisons were made using 2-tailed Student's t test (A). All data are mean  $\pm$  SEM. \* $P < 0.05$ .

## Supplemental Figure 2

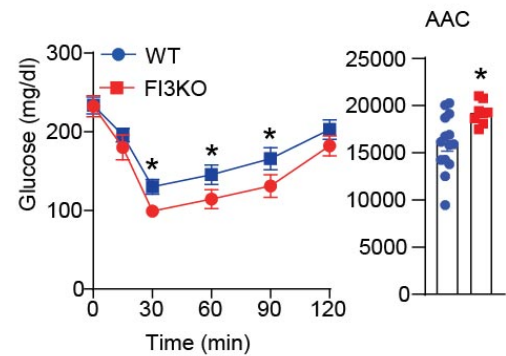
**A**



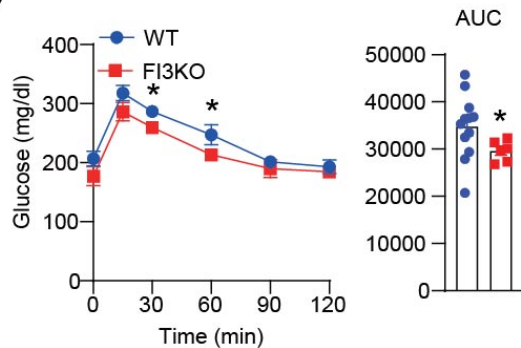
**B**



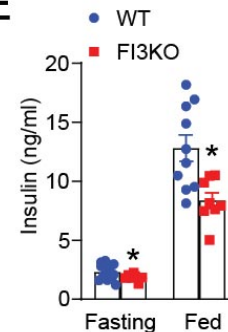
**C**



**D**

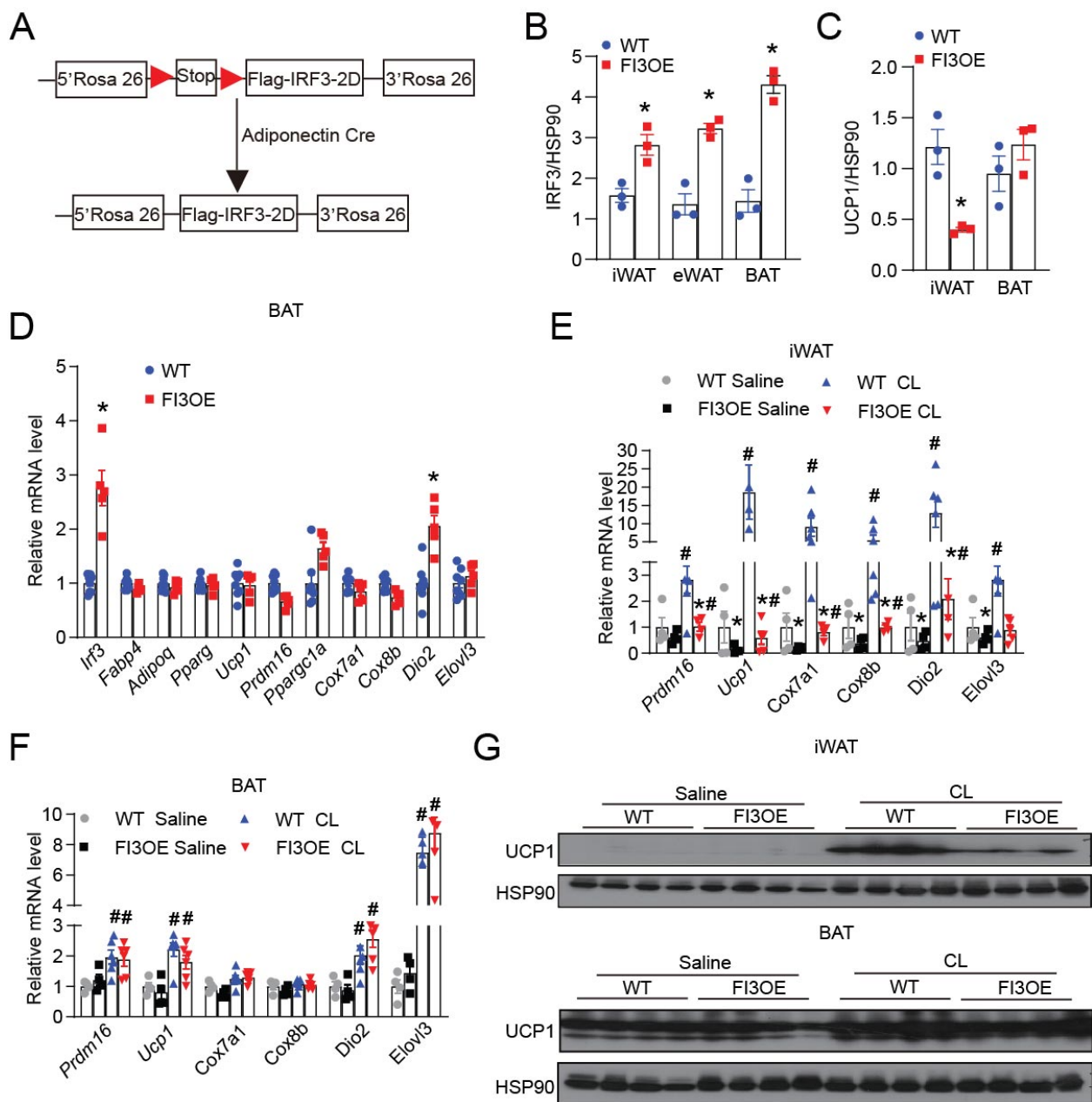


**E**



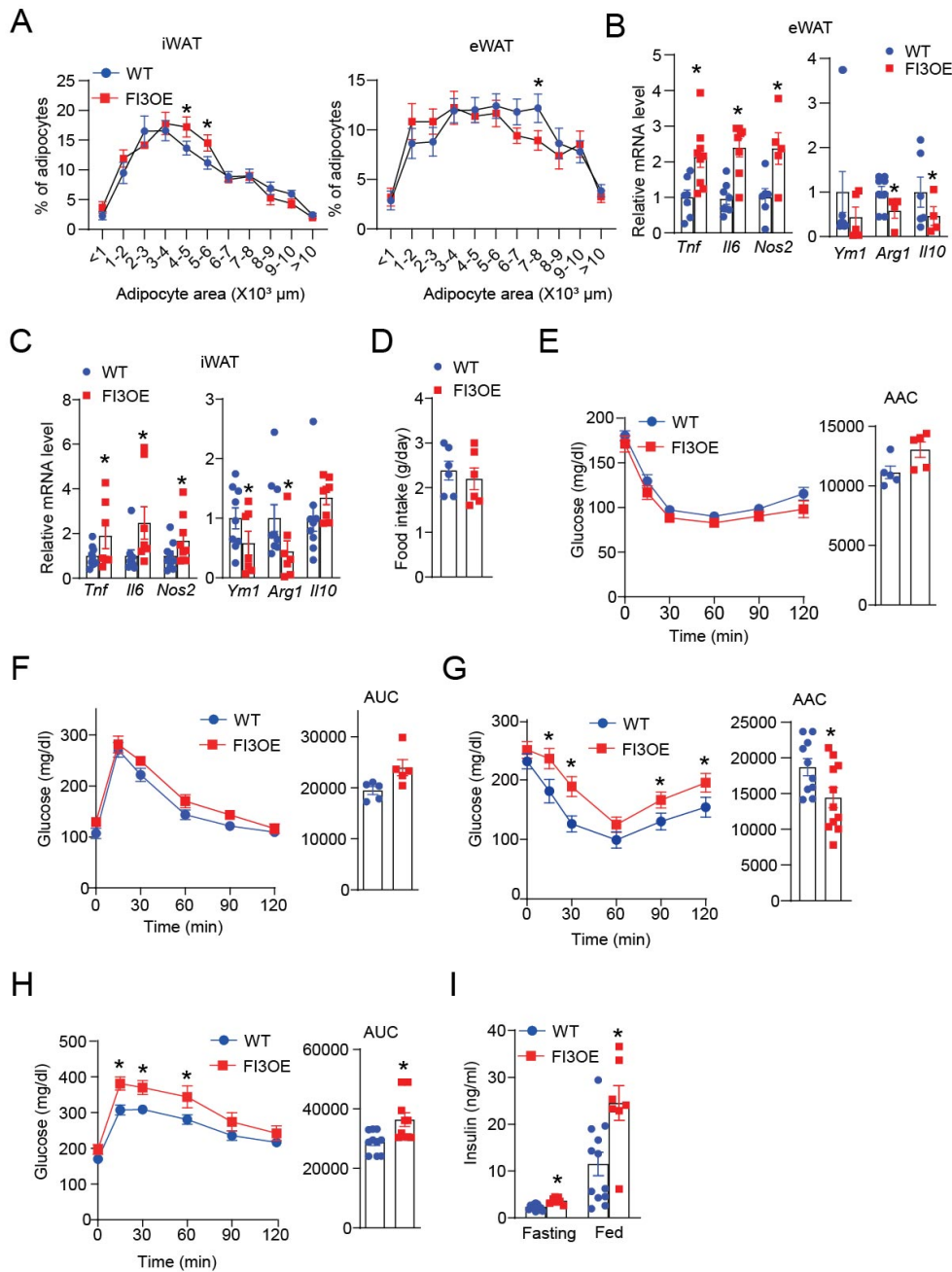
**Supplemental Figure 2. Adipocyte-specific IRF3 deficiency attenuates HFD-induced obesity.** (A) Analysis of adipocyte size of iWAT and eWAT in mice described as Figure 2D (n=6-10). (B) Oxygen consumption of WT and FI3KO mice after 4 weeks HFD feeding (n=8-10). (C) Insulin tolerance test (ITT) performed in WT and FI3KO mice after 16 weeks on HFD. Right panel: Area above the curve of ITT (n=8-10). (D) Glucose tolerance test (GTT) performed in WT and FI3KO mice after 16 weeks on HFD. Right panel: Area under the curve of GTT (n=8-10). (E) Fed and fasting plasma insulin levels in WT and FI3KO mice after 9 weeks on HFD (n=8-10). Statistical comparisons were made using two-way ANOVA (A, C and D) or 2-tailed Student's t test (B and E). Data presented as mean  $\pm$  SEM, \* $P$ <0.05.

### Supplemental Figure 3



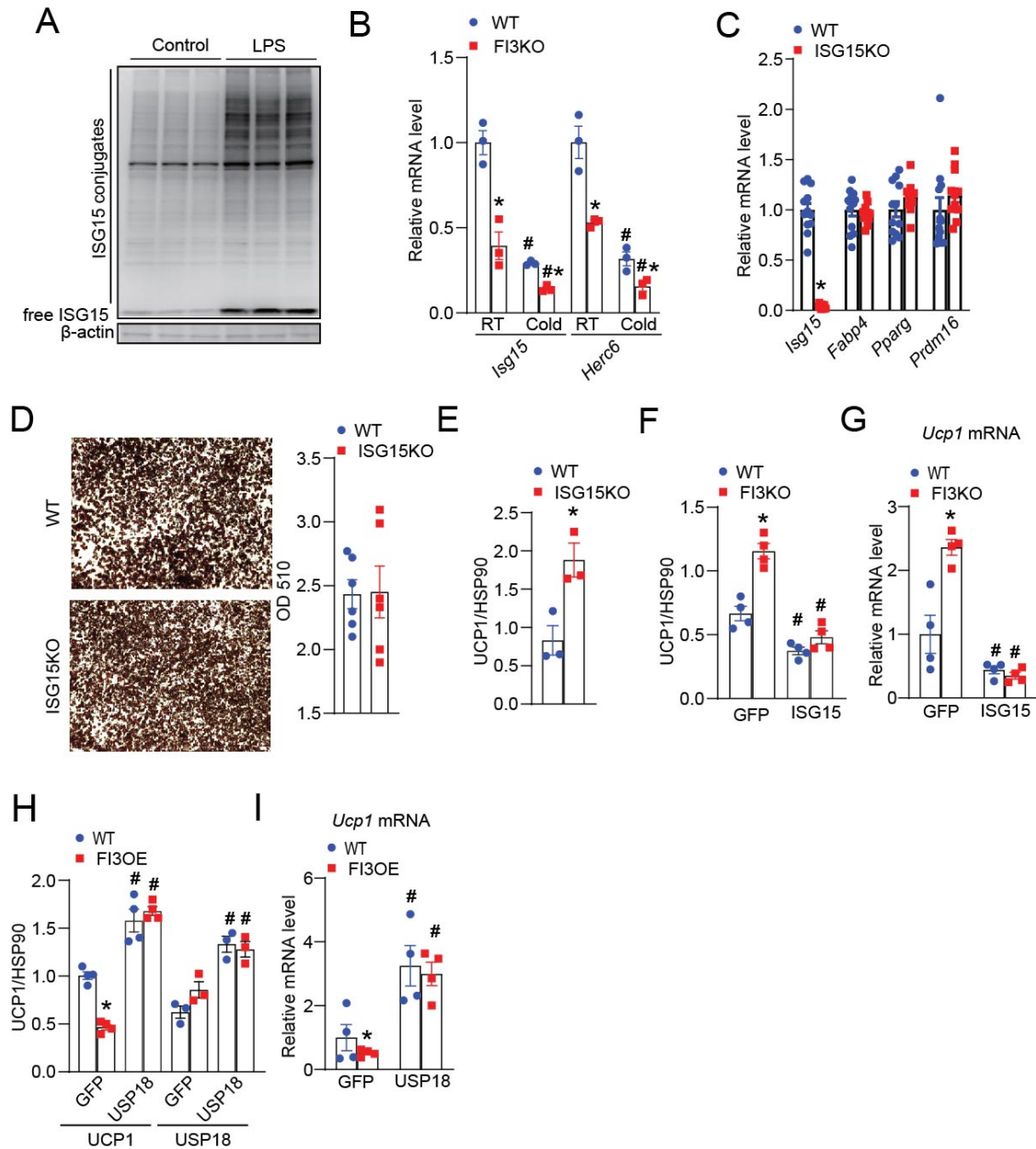
**Supplemental Figure 3. Adipocyte-specific IRF3 overexpression suppresses thermogenesis.** (A) Schematic diagram showing generation of FI3OE mice. (B) Quantification of IRF3 western blot band intensity as described in Figure 3B (n=3). (C) Quantification of UCP1 western blot band intensity as described in Figure 3C (n=3). (D) Thermogenic gene expression in BAT of chow-fed WT and FI3OE mice after 7 days cold challenge (n=8-10). (E and F) Thermogenic gene expression in iWAT (E) and BAT (F) of chow-fed WT and FI3OE mice 5 days after saline or (1mg/kg) CL 316,243 administration (n=8-10). (G) Western blot of UCP1 in iWAT of mice described in (E) and (F) (n=3 each group). Statistical comparisons were made 2-tailed Student's t test (B-F). Data presented as mean  $\pm$  SEM, \* $P$ <0.05 vs. WT; # $P$ <0.05 vs. saline.

Supplemental Figure 4



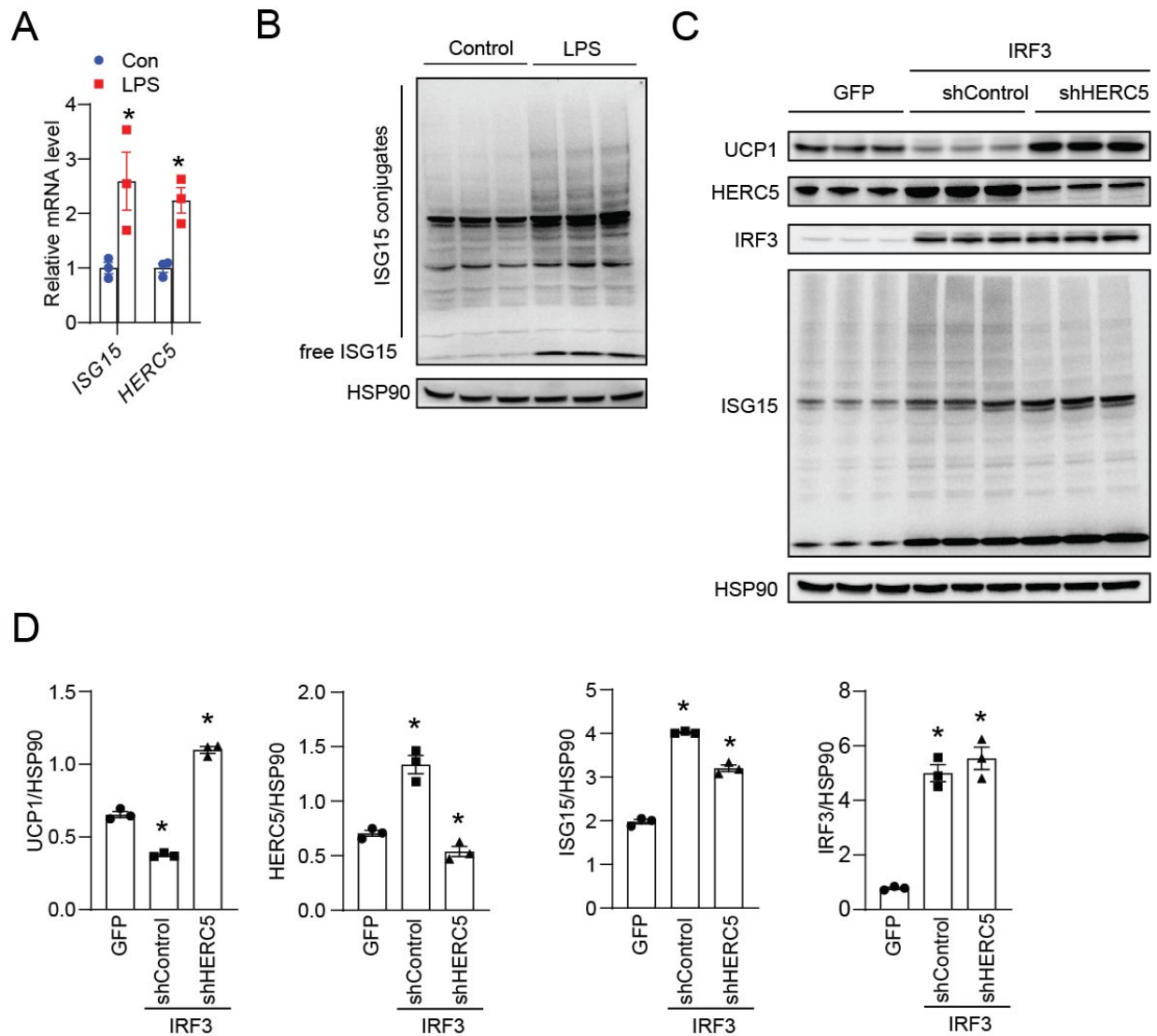
**Supplemental Figure 4. Adipocyte-specific IRF3 overexpression increases HFD-induced insulin resistance.** (A) Analysis of adipocyte size of iWAT and eWAT in mice described as Figure 4F (n=6-8). (B and C) mRNA levels of M1 and M2 macrophage marker genes in SVF from eWAT (B) and iWAT (C) of mice after 16 weeks HFD feeding (n=8-10). (D-F) Food intake (D), Insulin tolerance test (E) and glucose tolerance test (F) of 12-week old chow-fed WT and FI3KO male mice (n=6 each group). (G) Insulin tolerance test (ITT) performed in WT and FI3OE mice after 16 weeks on HFD. Right panel: Area above the curve of ITT (n=8-10). (H) Glucose tolerance test (GTT) performed in WT and FI3OE mice after 16 weeks on HFD. Right panel: Area under the curve of GTT (n=8-10). (I) Fed and fasting plasma insulin levels in WT and FI3KO mice after 6 weeks on HFD (n=8-10). Statistical comparisons were made using two-way ANOVA (A, G and H) or 2-tailed Student's t test (B, C and I). Data are presented as mean  $\pm$  SEM. \* $P$ <0.05.

Supplemental Figure 5



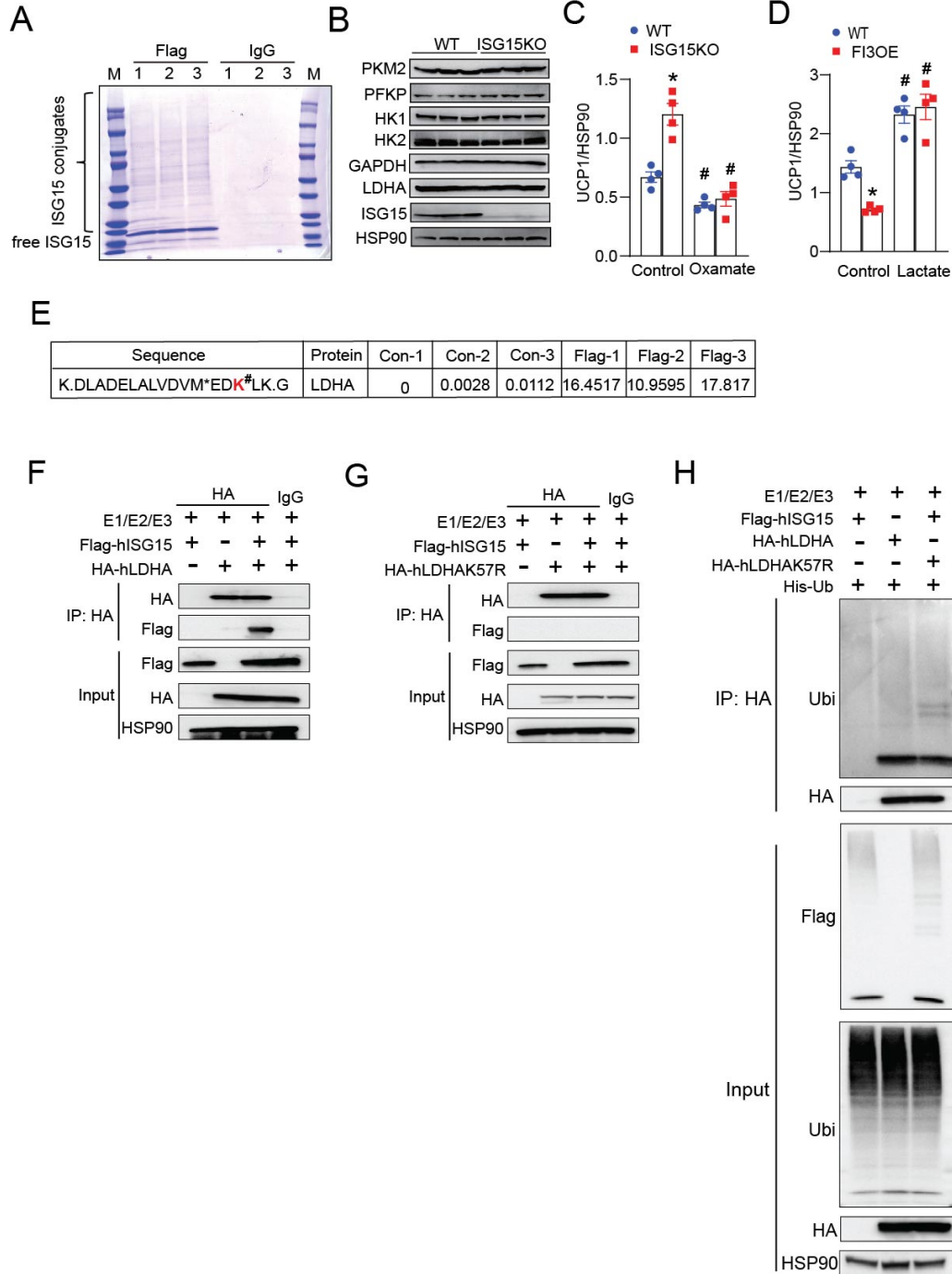
**Supplemental Figure 5. ISG15 does not affect beige adipogenesis *in vitro*.** (A) Western blot of free ISG15 and ISG15 conjugates in primary adipocytes treated with vehicle or LPS (100ng/ml) for 12h. (B) mRNA levels of *Isg15* and *Herc6* in primary adipocytes from iWAT in 12-week old male chow-fed WT and FI3KO mice from room temperature and cold challenge (n=3). (C) mRNA analysis of indicated genes in WT and *Isg15*<sup>-/-</sup> beige adipocytes (n=3). (D) Oil Red O staining of WT and *Isg15*<sup>-/-</sup> beige adipocytes (n=3). (E and F) Quantification of UCP1 western blot band intensity as described in Figure 5D (E) and Figure 5G (F) (n=3). (G) mRNA levels of *Ucp1* in primary adipocytes as described in Figure 5G (n=3). (H) Quantification of UCP1 western blot band intensity as described in Figure 5I (n=3). (I) mRNA levels of *Ucp1* in primary adipocytes as described in Figure 5I (n=3). Statistical comparisons were made using 2-tailed Student's t test (B, C and E-I). Data are presented as mean ± SEM. \*P<0.05 vs. WT; #P<0.05 vs. RT.

Supplemental Figure 6



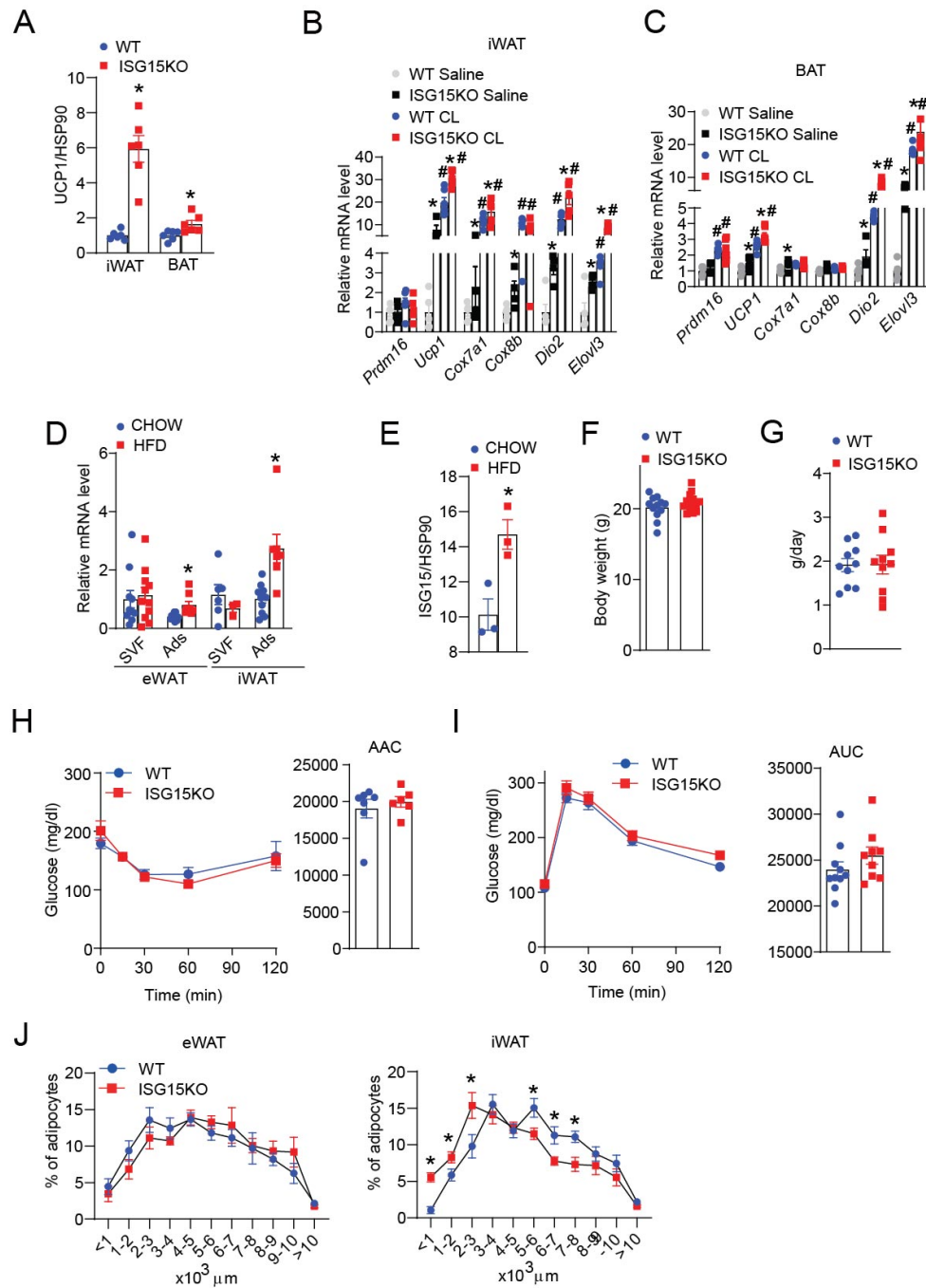
**Supplemental Figure 6. IRF3 suppresses thermogenesis in human thermogenic adipocytes through ISG15.** (A) mRNA levels of *Isg15* and *Herc6* in primary human thermogenic adipocytes treated with control or LPS (100ng/ml) for 12h (n=3). (B) Western blot of free ISG15 and ISG15 conjugates in primary human thermogenic adipocytes treated with vehicle or LPS (100ng/ml) for 12h (n=3). (C and D) Western blot of UCP1, HERC5, IRF3 and ISG15 in primary human thermogenic adipocytes infected with indicated virus (n=3). Statistical comparisons were made using 2-tailed Student's t test (A and D). Data are presented as mean  $\pm$  SEM. \* $P < 0.05$ .

Supplemental Figure 7



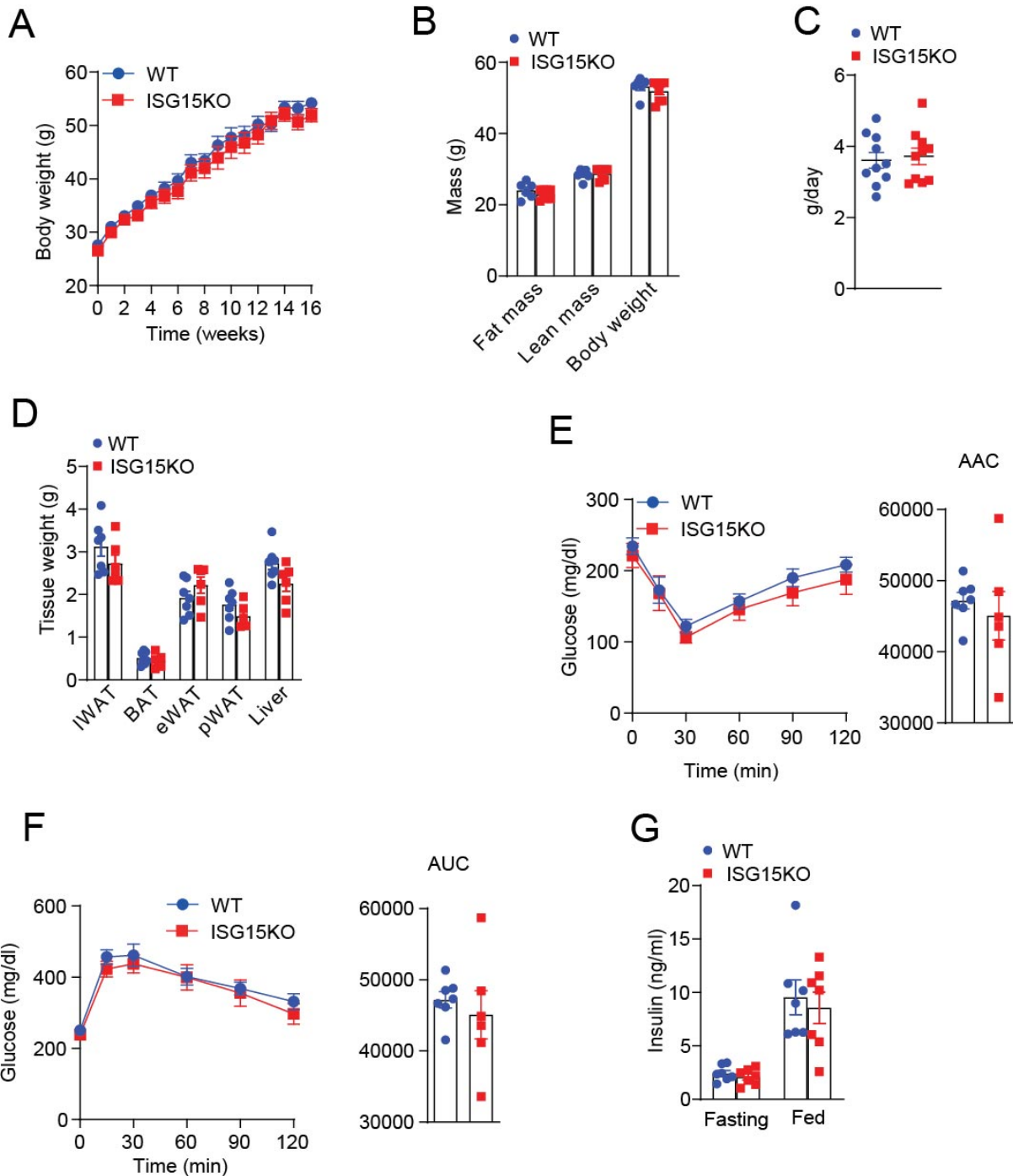
**Supplemental Figure 7. ISGylation suppresses LDHA activity.** (A) Coomassie staining of free ISG15 and ISGylated proteins prior to proteomic analysis (n=3). (B) Western blot of glycolytic enzymes in WT and *Isg15*<sup>-/-</sup> beige adipocytes. (C and D) Quantification of UCP1 western blot band intensity as described in Figure 8A (A) and Figure 8B (B) (n=4). (E) Illustration of ISGylation sites in LDHA protein. (F-H) HEK293T cells were transfected with the indicated plasmids. Twenty-four hrs after transfection, cell lysates were immunoprecipitated with an anti-HA antibody (F-H) and then immunoblotted with the indicated antibodies. Statistical comparisons were made using 2-tailed Student's t test. Data are presented as mean  $\pm$  SEM. \* $P < 0.05$  vs. WT; # $P < 0.05$  vs. Control.

Supplemental Figure 8



**Supplemental Figure 8. *Isg15*<sup>-/-</sup> mice display increased thermogenesis.** (A) Quantification of UCP1 western blot band intensity as described in Figure 9D (n=4). (B and C) Thermogenic gene expression in iWAT (B) and BAT (C) of chow-fed WT and *Isg15*<sup>-/-</sup> mice after saline or CL 316,243 administration (n=8-10). (D) *Isg15* mRNA in isolated SVF and adipocyte fractions from eWAT and iWAT of male mice fed chow or HFD (n=6). (E) Quantification of ISG15 western blot band intensity as described in Figure 11B (n=3). (F-I) Body weight (F), Food intake (G), Insulin tolerance test (H) and glucose tolerance test (I) of 12-week old male chow-fed WT and *Isg15*<sup>-/-</sup> male mice (n=6). (J) Analysis of adipocyte size of iWAT and eWAT in mice described as Figure 11F (n=6-8). Statistical comparisons were made using ANOVA (I) or 2-tailed Student's t test (A-E). Data are presented as mean ± SEM, \*P<0.05 vs. WT; #P<0.05 vs. saline.

## Supplemental Figure 9



**Supplemental Figure 9. Metabolic profile of WT and *Isg15*<sup>-/-</sup> mice on HFD at thermoneutrality.** (A) Body weight of male WT and *Isg15*<sup>-/-</sup> mice during HFD feeding at thermoneutrality (n=8-10). (B-D) Body composition (B), food intake (C) and fat mass (D) of male WT and *Isg15*<sup>-/-</sup> mice after 16 weeks HFD feeding at thermoneutrality (n=8-10). (E) Insulin tolerance test (ITT) performed in mice as described as (B). Right panel: Area above the curve of ITT (n=8-10). (F) Glucose tolerance test (GTT) performed in mice as described as (B). Right panel: Area under the curve of GTT (n=8-10). (G) Fed and fasting plasma insulin levels in mice as described as (B) (n=8-10). Data are presented as mean ± SEM.

# Gel source data-1

Figure1

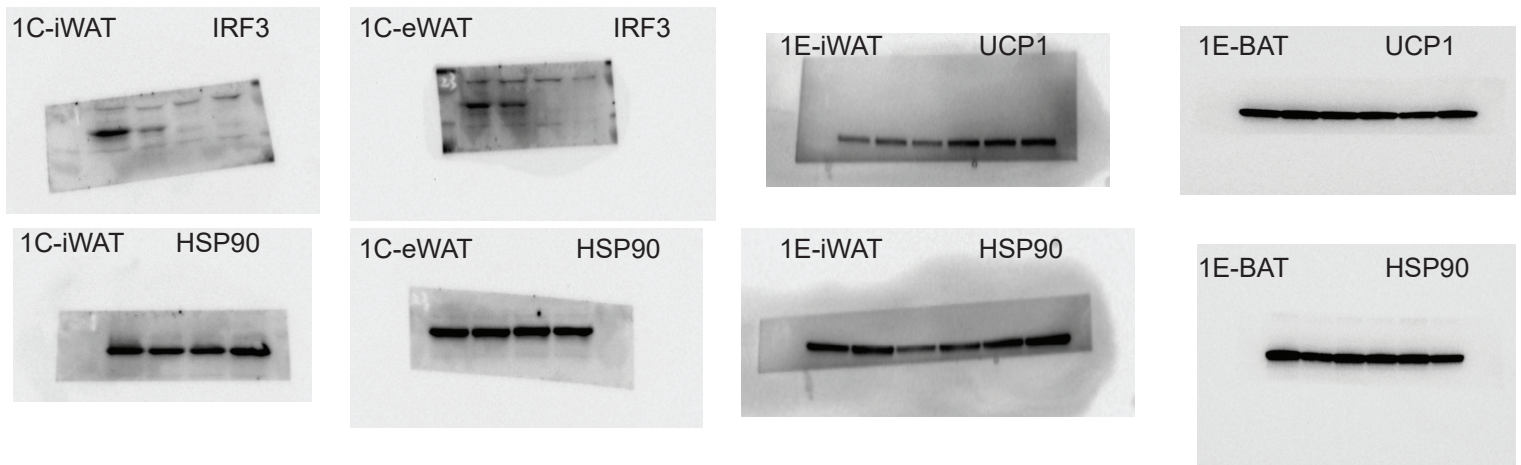


Figure3

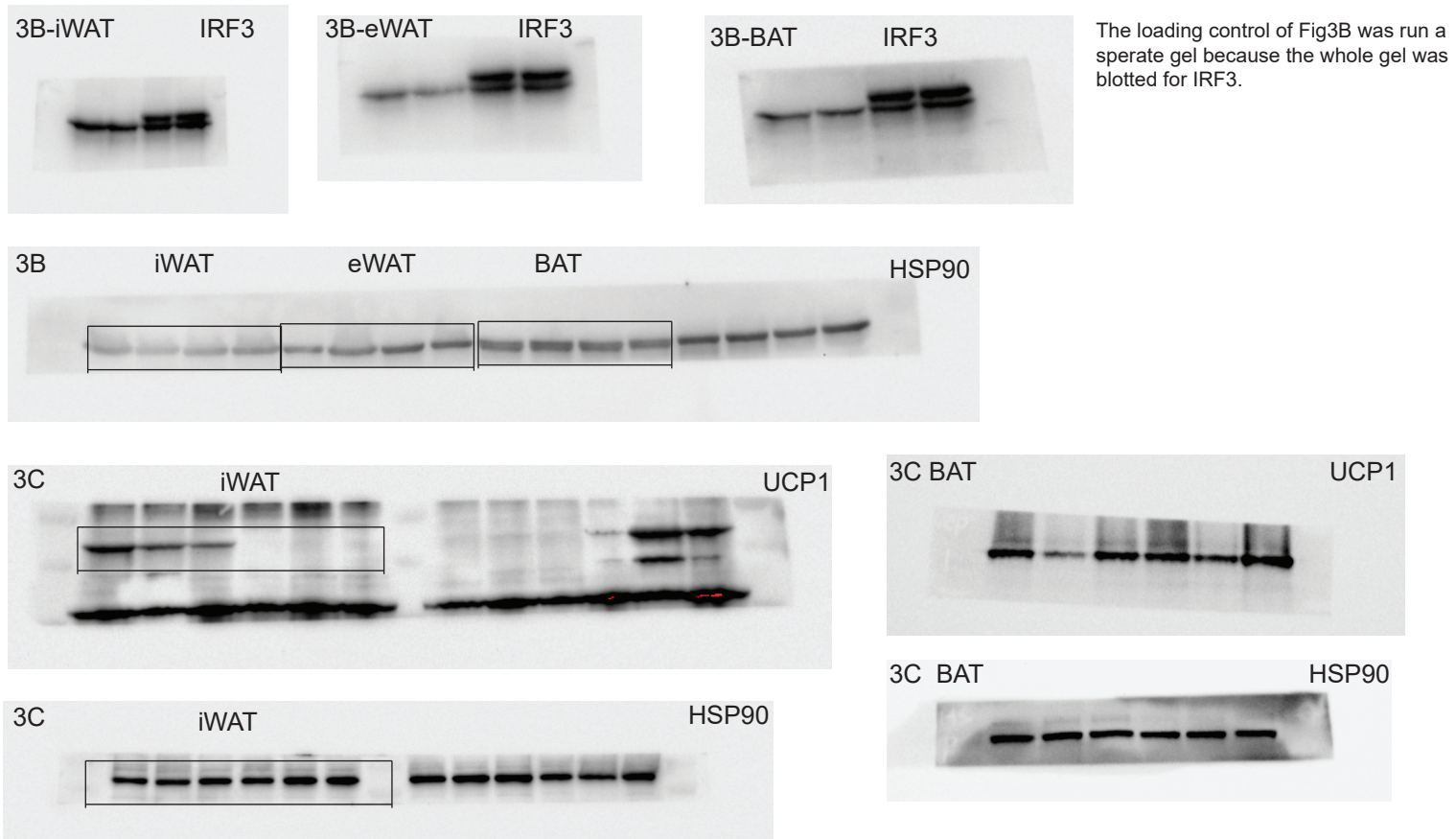


Figure5

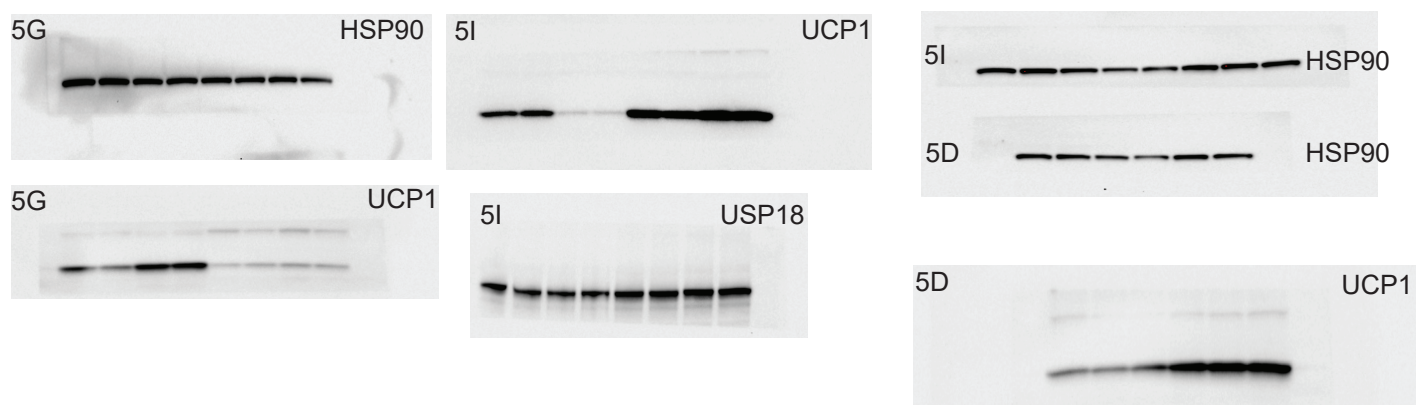


Figure 6

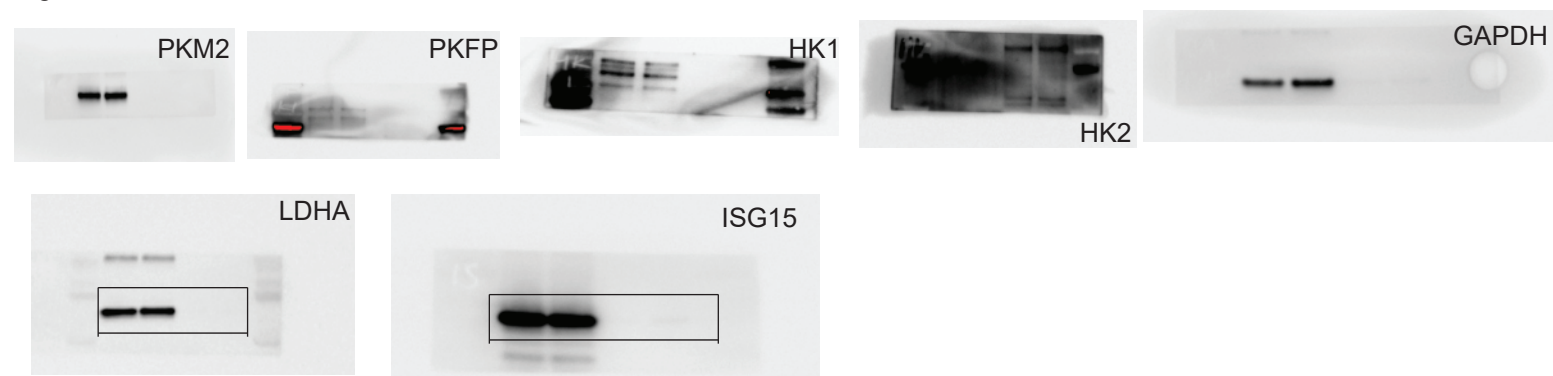


Figure 8

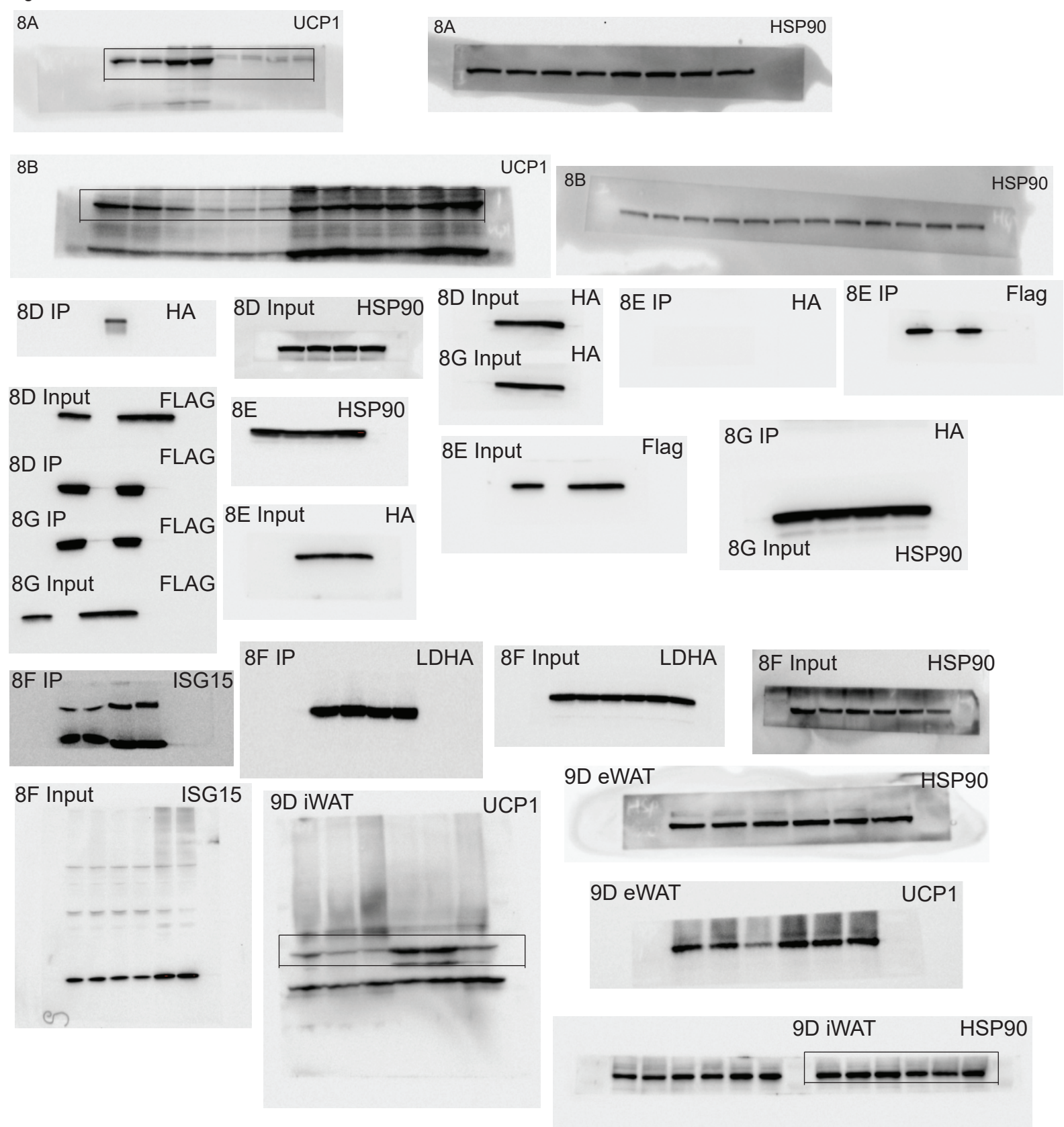


Figure 10

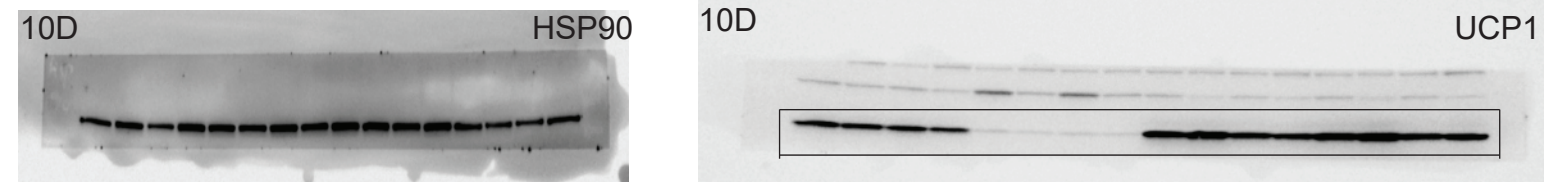
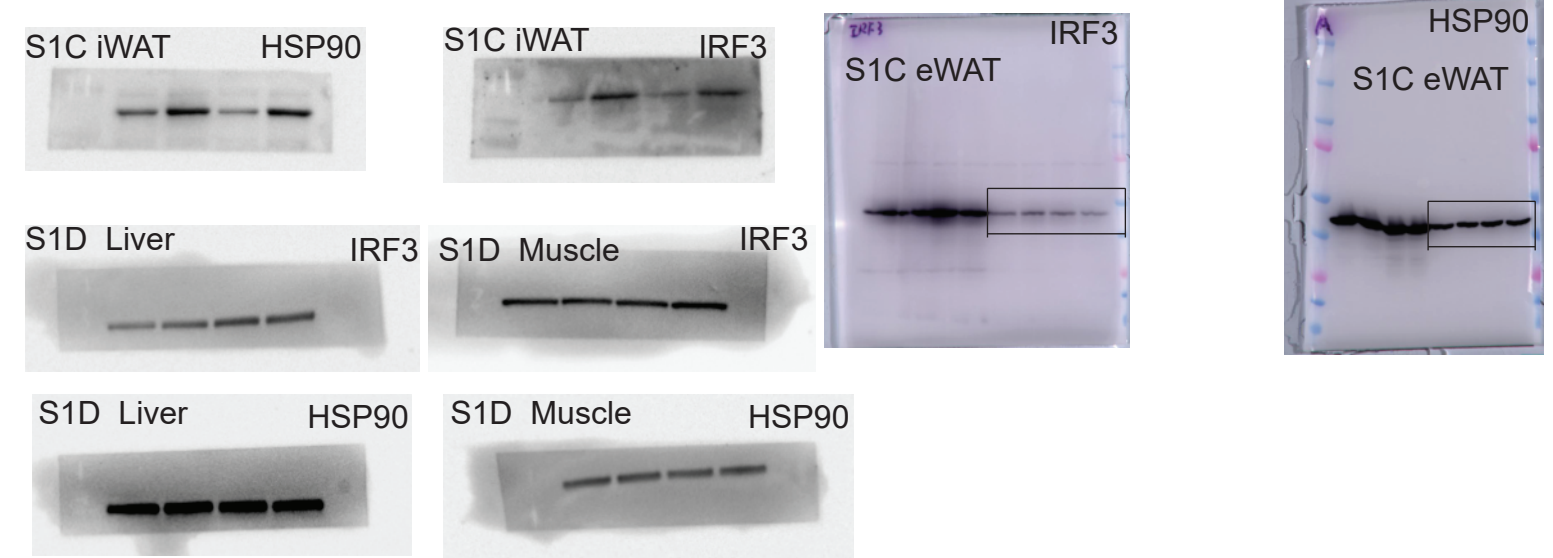


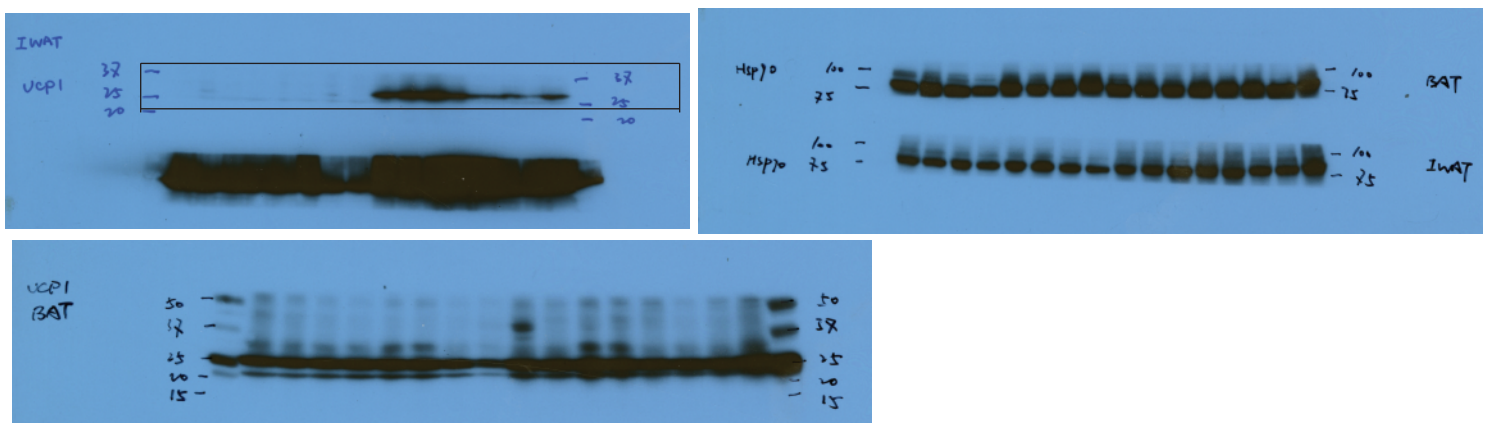
Figure 11



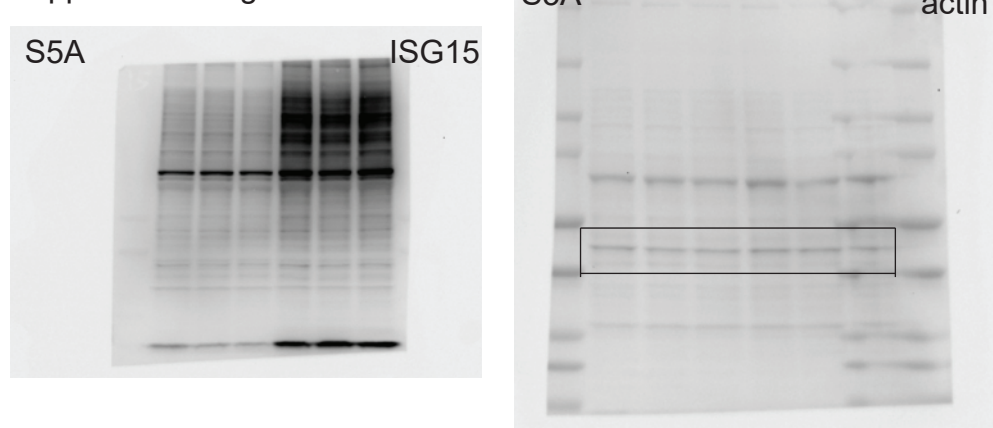
Supplemental Figure1

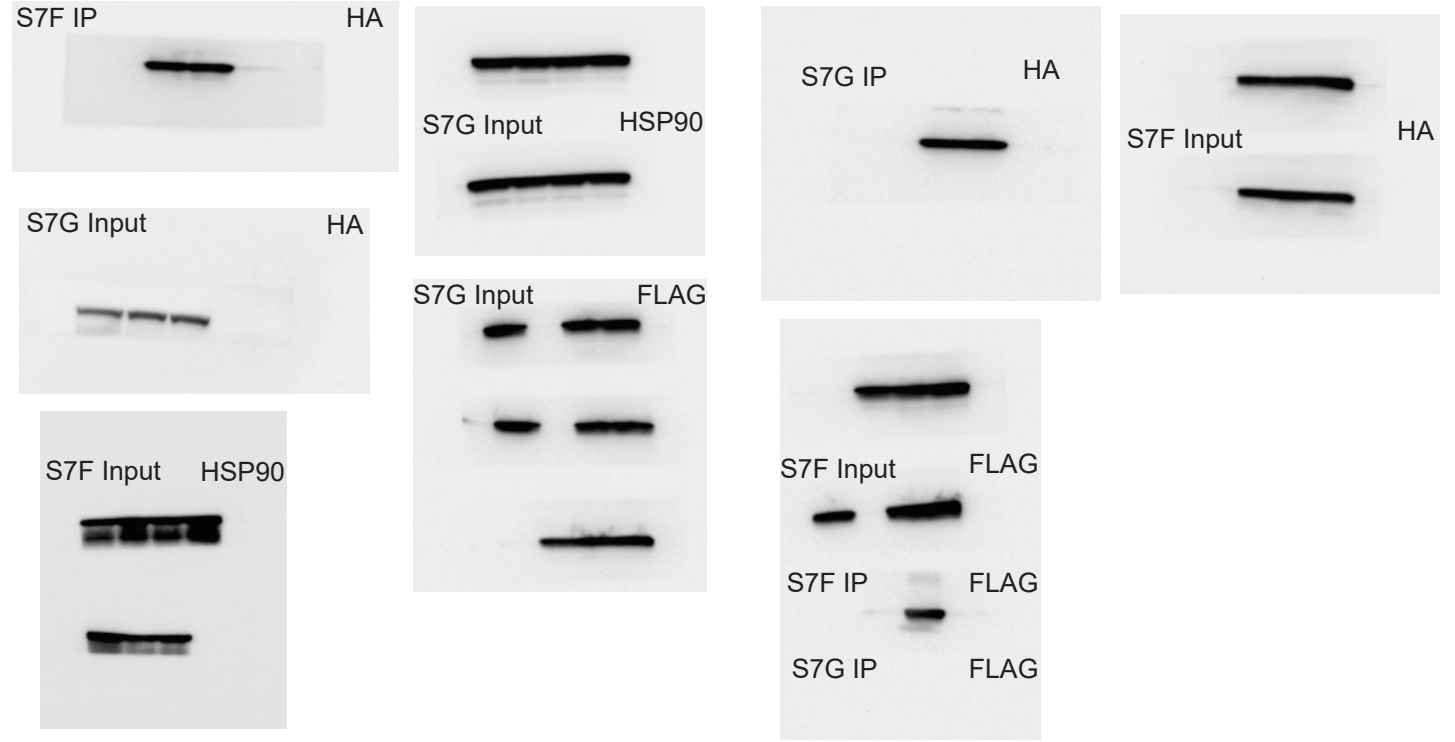
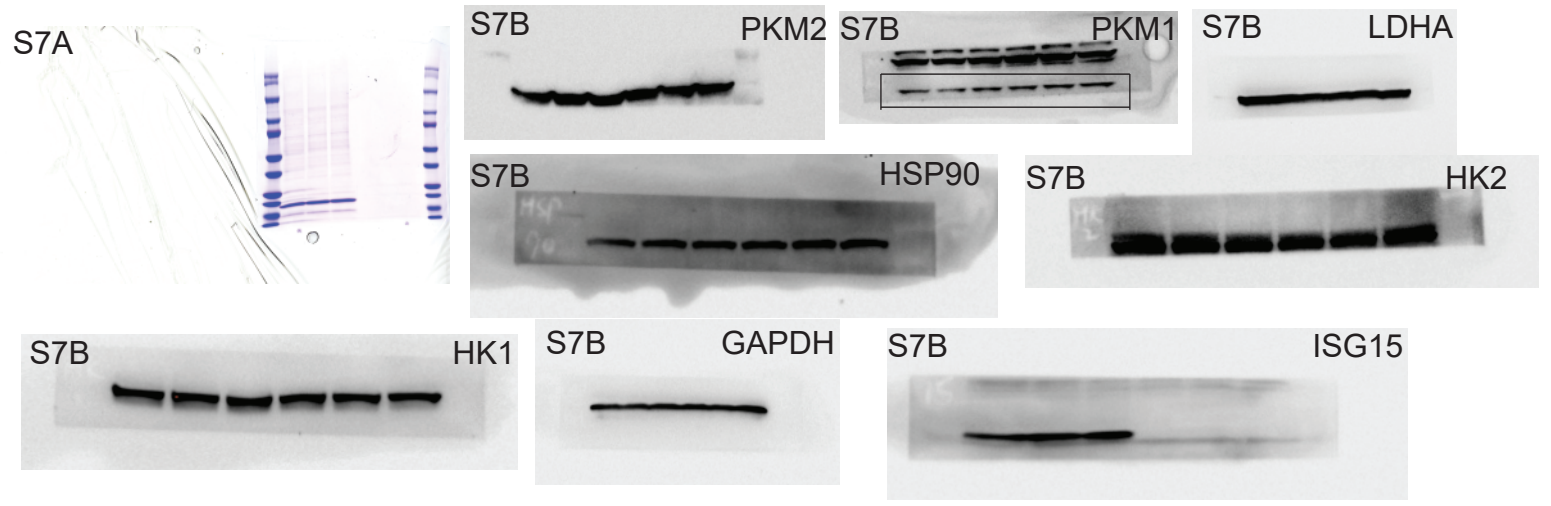
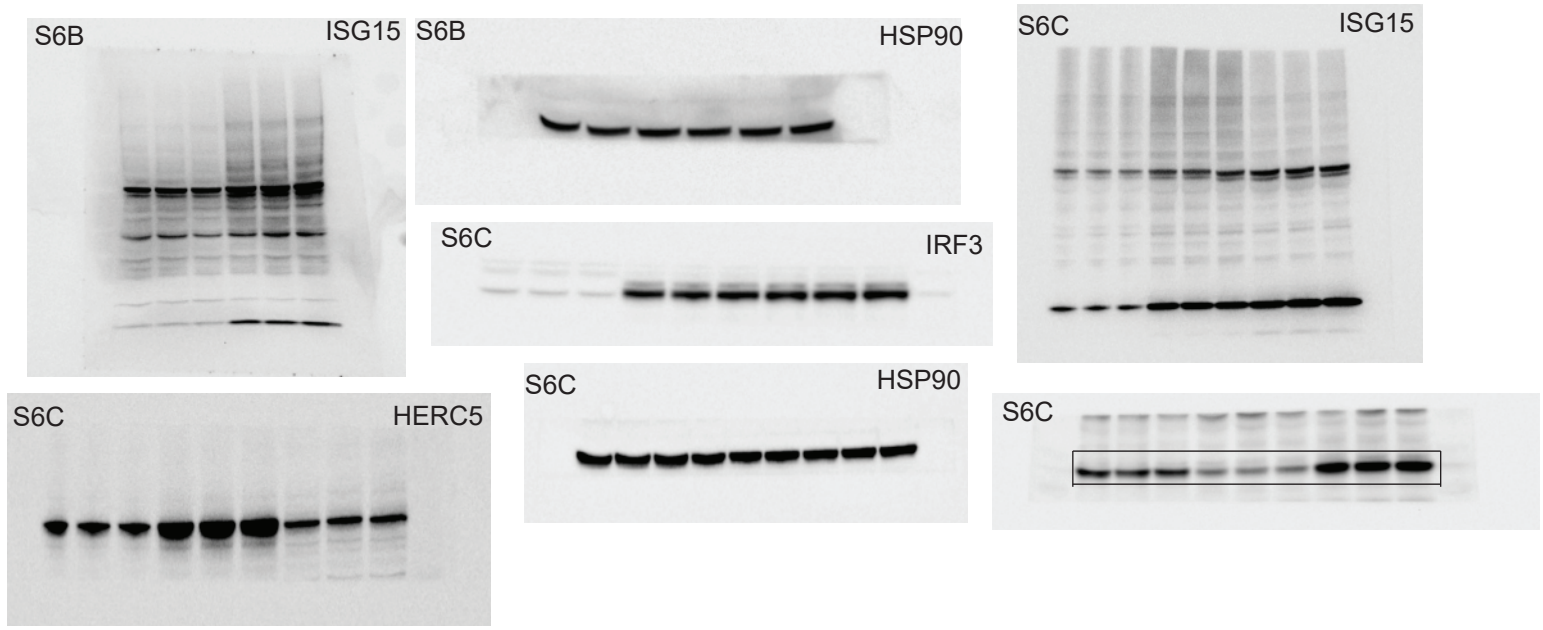


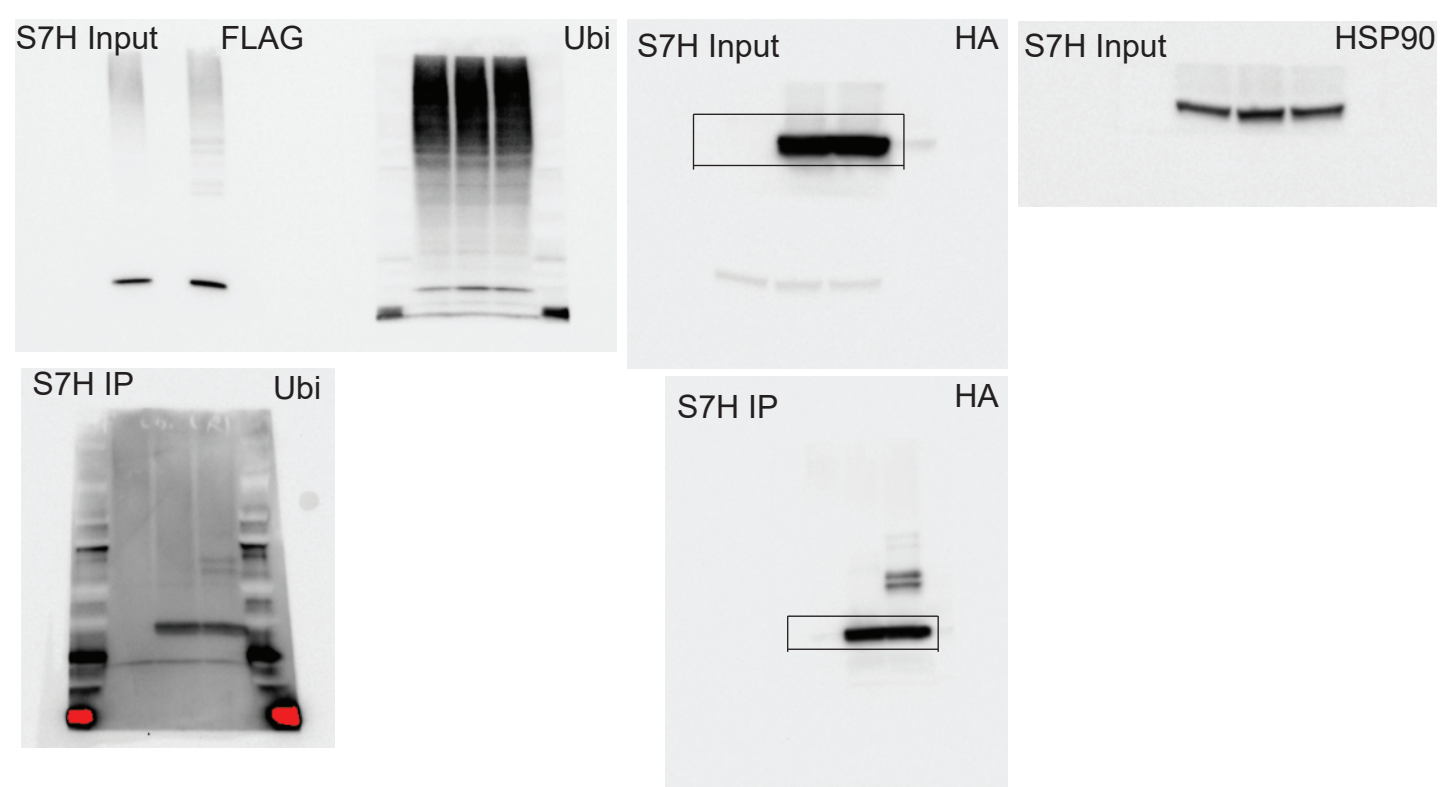
Supplemental Figure3



Supplemental Figure5







Supplemental Table 1. RNA-seq results from eWAT of FI3OE mice

Supplemental Table 2. Results of mass spectrometry analysis of ISGylated proteins in cultured adipocytes

Supplemental Table 3. Characteristics of human subjects

Supplemental Table 4. Primer sequences used in this study

## Supplemental References

1. Kumari M, Wang X, Lantier L, Lyubetskaya A, Eguchi J, Kang S, et al. IRF3 promotes adipose inflammation and insulin resistance and represses browning. *J Clin Invest*. 2016;126(8):2839-54.
2. Roh HC, Tsai LT, Lyubetskaya A, Tenen D, Kumari M, and Rosen ED. Simultaneous Transcriptional and Epigenomic Profiling from Specific Cell Types within Heterogeneous Tissues In Vivo. *Cell Rep*. 2017;18(4):1048-61.
3. Kang S, Kong X, and Rosen ED. Adipocyte-specific transgenic and knockout models. *Methods Enzymol*. 2014;537:1-16.
4. Kim D, Langmead B, and Salzberg SL. HISAT: a fast spliced aligner with low memory requirements. *Nature methods*. 2015;12(4):357-60.
5. Liao Y, Smyth GK, and Shi W. featureCounts: an efficient general purpose program for assigning sequence reads to genomic features. *Bioinformatics*. 2014;30(7):923-30.
6. Robinson MD, McCarthy DJ, and Smyth GK. edgeR: a Bioconductor package for differential expression analysis of digital gene expression data. *Bioinformatics*. 2010;26(1):139-40.
7. Huang da W, Sherman BT, and Lempicki RA. Bioinformatics enrichment tools: paths toward the comprehensive functional analysis of large gene lists. *Nucleic acids research*. 2009;37(1):1-13.
8. Yan S, Zhang Q, Zhong X, Tang J, Wang Y, Yu J, et al. I prostanoid receptor-mediated inflammatory pathway promotes hepatic gluconeogenesis through activation of PKA and inhibition of AKT. *Diabetes*. 2014;63(9):2911-23.
9. Ting L, Rad R, Gygi SP, and Haas W. MS3 eliminates ratio distortion in isobaric multiplexed quantitative proteomics. *Nat Methods*. 2011;8(11):937-40.